Acta Cryst. (1956). 9, 16

Growth Features on Crystals of Long-Chain Compounds. II

BY S. AMELINCKX

Laboratorium voor Kristalkunde, Rozier 6, *Gent, Belgium*

(*Received* 30 *March* 1955)

Growth features observed on crystals of the orthorhombic modification of the *n*-alcohols $C_{22}H_{43}OH$, $C_{24}H_{49}OH$ and $C_{26}H_{53}OH$ are described. They consist of interlaced spirals of two types. The influence of the presence of imperfect dislocations on the growth patterns is discussed. It has been possible to conclude that growth round an imperfect dislocation in a crystal of the orthorhombic modification of the *n*-alcohols does *not* produce a polytype. The normal stacking is continued; this causes certain complications in the growth pattern.

The growth of twinned crystals of *n*-alcohols and monocarboxylic acids (behenic, eikosanic and lignoceric acid) is considered. A growth mechanism for ordinary twins and for certain polysynthetic twins is proposed.

1. Introduction

In the first part of this paper (Amelinckx, 1955) growth features on crystals of the β-form of the *n*-alcohols ($C_{22}H_{45}OH$, $C_{24}H_{49}OH$ and $C_{26}H_{53}OH$) have been discussed with special reference to polytypism. In this second part the growth patterns observed on the α-form (orthorhombic) of the *n*-alcohols will be described and special attention will be given to imperfect dislocations, which are relatively frequent in long-chain compounds.

We also discuss some observations on twinning of crystals of the *n*-alcohols and of monocarboxylic acids (eikosanic, behenic and lignoceric acid). A detailed account concerning growth features on this last series of compounds will be given in Part III.

2. Growth features on crystals of the *n*-alcohols

Whereas in Part I the β-form has been considered in some detail we will now deal with the growth patterns of the α-form, which is orthorhombic.

2·1. *Growth round perfect dislocations on crystals of the α-form*

2·1·1. *Introduction*

Crystals of this form only present well formed interlaced patterns. They belong to two distinct types, shown on Fig. 1(*a*, *b*) and Fig. 1(*c*, *d*). The developed fronts have the orientations [110], and occasionally also [010].

The heights of the main growth fronts, measured by means of multiple-beam interferometry (method of doubly silvered films (Tolansky, 1948)) indicate that these are bimolecular in both cases. The 'interlacings' are consequently monomolecular, and the bimolecular nature of the growth fronts results from the grouping of monolayer fronts. When the central dislocation has a large Burgers vector, dissociation of the spiral step into multiple interlaced spirals generally occurs (under the growth conditions used); Fig. 1(*a*) is an example of a fourfold interlaced spiral.

The interlaced character of the spirals has in this case no direct relation with polytypism but is simply a consequence of the difference in polar diagram of successive monomolecular layers. We will now analyse in some detail the growth patterns of both types.

2·1·2. *Interlaced spiral of type* 1 (*Figs.* 1(*b*) *and* 6)

Deductions, similar to the ones made in Part I, prove that the simple interlaced spiral consists in fact of two single spirals (*A* and *B*), as shown in Fig. 1. The composition can be represented in the following way:

Sector	1	2	3	4	1
Composition	*A*	*B*	*B*	*A*	*A*
		↗		↗	
	B	*A*	*A*	*B*	*B*

From the geometry of the growth pattern it will be clear that the bonding between the substrate and the growing layer is of the OH–OH type in one half of the spiral (e.g. in sectors 1 and 4) and of the CH_3–CH_3 type in the other sectors.

The polar diagram of each monolayer can be determined only partly from the growth pattern. This is due to the fact that we can deduce the growth velocity for a given layer only in those directions for which that particular layer is rate-determining. The observed equality of the spacings in 1 and 2 and in 3 and 4 is expressed, by means of the following relations:

$$^1v_B = {}^2v_A \ (1)\,, \quad {}^3v_A = {}^4v_B \ (2)$$

(^1v_A means the growth velocity of layer *A* in sector 1).

The interlacing further proves that:

$$^1v_A \geqslant {}^1v_B \ (3)\,, \quad {}^3v_B \geqslant {}^3v_A \ (5)\,,$$
$$^2v_B > {}^2v_A \ (4)\,, \quad {}^4v_A > {}^4v_B \ (6)\,.$$

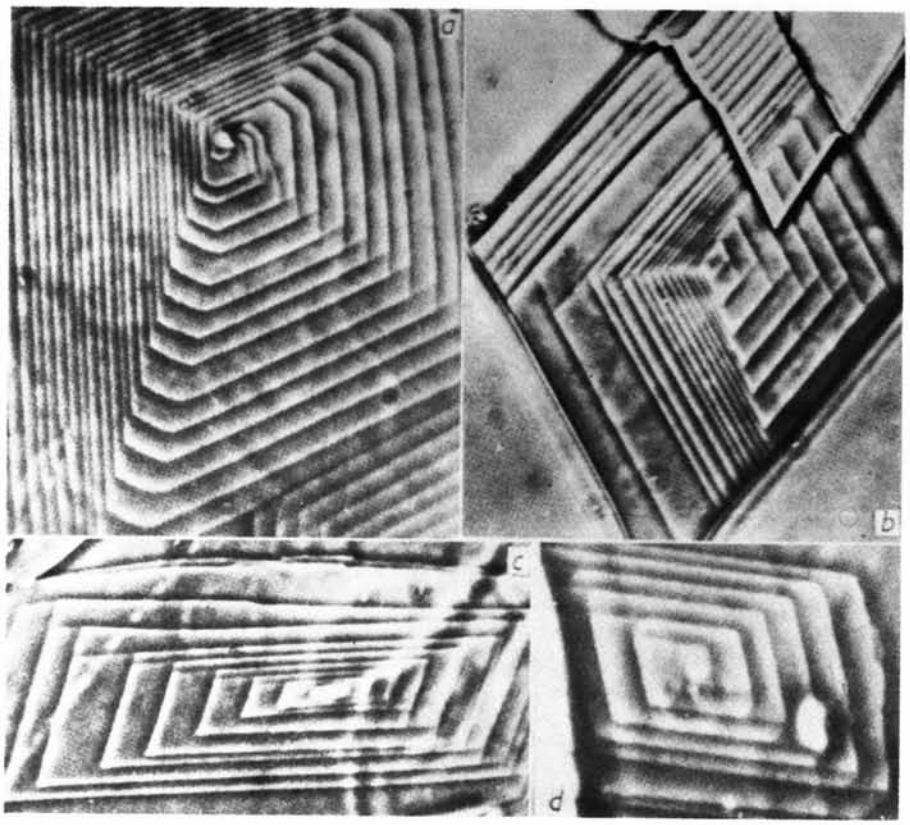

Fig. 1. Interlaced spirals on crystals of the α-form of the *n*-alcohols. (*a*) Fourfold interlaced spiral of type 1 (1000×). (*b*) Double interlaced spiral of type 1 (1000×). (*c*) Single interlaced spiral of type 2 (800×). (*d*) Single interlaced spiral of type 2 (1300×).

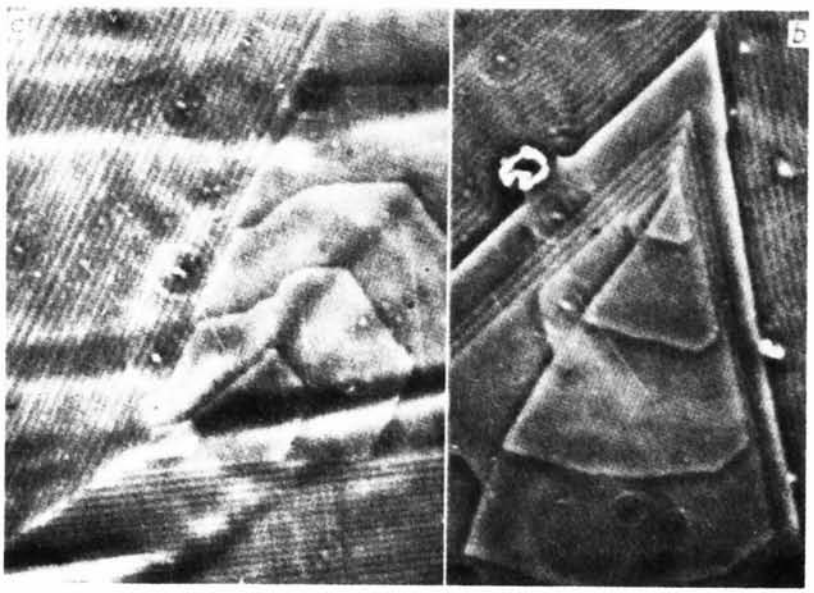

Fig. 2. Growth patterns due to growth round perfect dislocations in the presence of imperfect dislocations observed on crystals of the β-form of the *n*-alcohols ((*a*): 1400×; (*b*): 1000×).

[*To face p.* 16

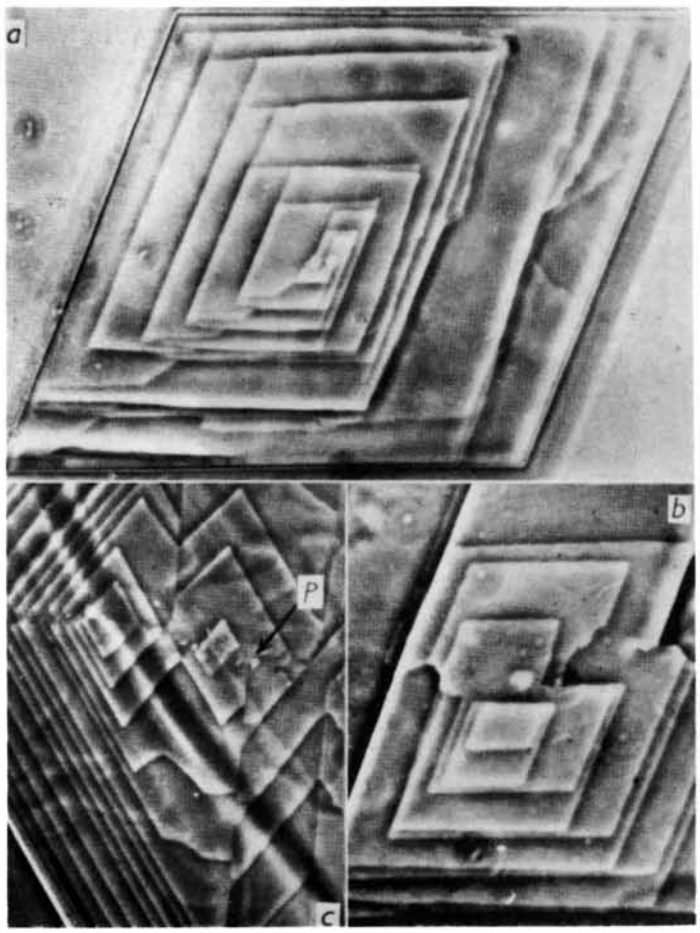

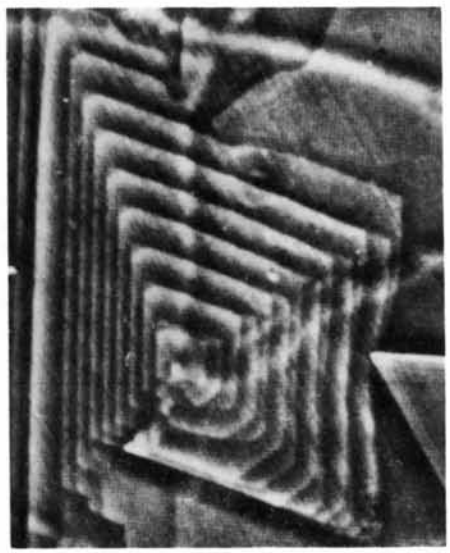

Fig. 3. Interlaced pattern due to growth round a half dislocation in crystal of the α-form of *n*-alcohols (1600×).

Fig. 4. (*a*) Interlaced pattern due to the growth round a dislocation of 2½ chain lengths. Kinks, due to the rearrangement of monomolecular fronts, clearly mark the trace of the misfit plane (1000×). (α-form.) (*b*) Growth pattern due to two half dislocations of opposite sign (950×). (α-form.) (*c*) Dominated imperfect dislocation in *P* (1000×).

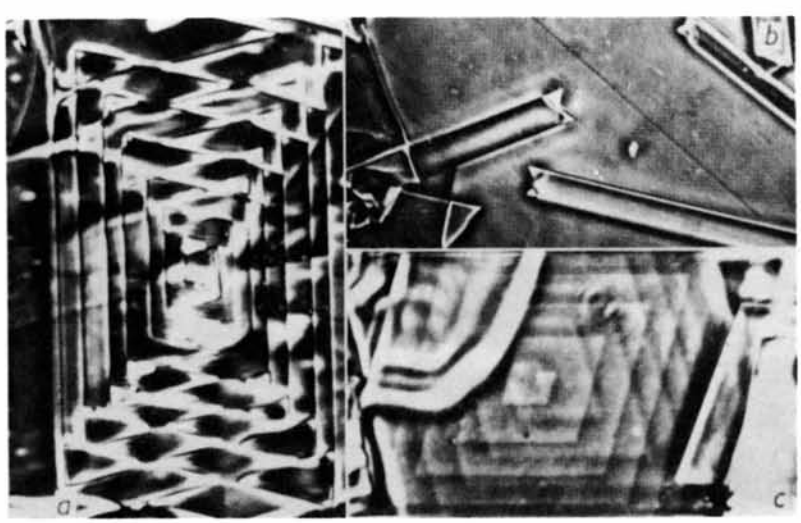

Fig. 5. (*a*) Polysynthetic twin of crystals of the *B*-form of behenic acid (1500×). (*b*) Contact twins of *n*-alcohol ($C_{24}H_{49}OH$) (900×). (*c*) Ordinary contact twin; *B*-form of lignoceric acid (1200×).

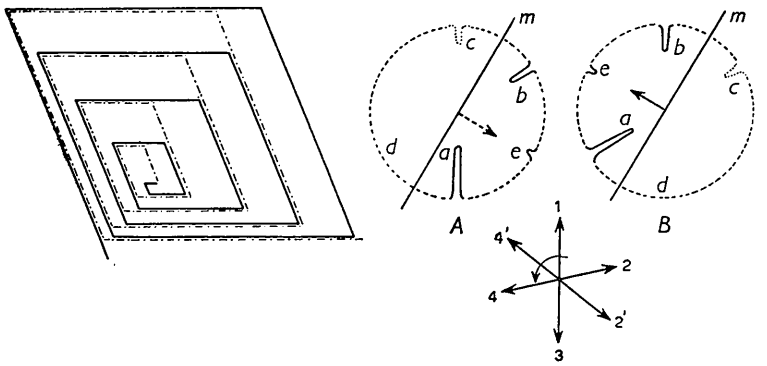

Fig. 6. Decomposition of the interlaced pattern of type 1 into single spirals.

Combination of (1) and (3) and of (2) and (6) gives

$$^1v_A \geqslant {}^2v_A\,, \qquad {}^4v_A > {}^3v_A\,.$$

From this we can conclude that the minima (*a*), (*b*), (*c*) and (*d*) of the polar diagram of layer *A* satisfy the following relations:

$$v_a < v_b \leqslant v_c\,; \qquad v_a < v_d\,.$$

The polar diagram of layer *A* belongs consequently to the symmetry class 1.

A similar argument leads to the conclusion that the polar diagram accounting for the behaviour of layer *B* can be derived from the one for *A* by taking the mirror image of it with respect to the short diagonal of the lozenge (*m*). The polar diagrams are shown in their hypothetical orientation in Fig. 6; one of them refers to a layer growing on a OH–OH bonding, the other to a layer growing on a CH_3–CH_3 bonding.

Reasoning in the same way as in Part I, it is easy to verify that correct interlacing and spacing is obtained when the layers grow according to their postulated polar diagram.

Although slightly differently shaped spirals of type 1 were observed, the symmetry relation between the two polar diagrams always holds. Fig. 1(*a*) gives an example. The pattern now consists of four interlaced spirals (i.e. eight monolayers) and growth fronts are developed also along [010].

2·1·3. *Type* 2 (*Figs.* 1(*c*) *and* 7)

This type of growth feature is less common than the first one. It is easy to show that the pattern is again composed of two simple monomolecular spirals, and the composition scheme is readily found:

Sector	1	2	3	4	1
Composition	*A*	*B*	*B*	*A*	*A*
	↗		↗		
	B	*A*	*A*	*B*	*B*

The resulting decomposition is indicated on Fig. 7.

Proceeding in the same way as for type 1, it can be shown that the behaviour of layer *A* can be described with a polar diagram similar to the one derived from type 1. The polar diagram for *B* is then related to the one for *A* by a rotation through 180°. This is also shown on Fig. 7.

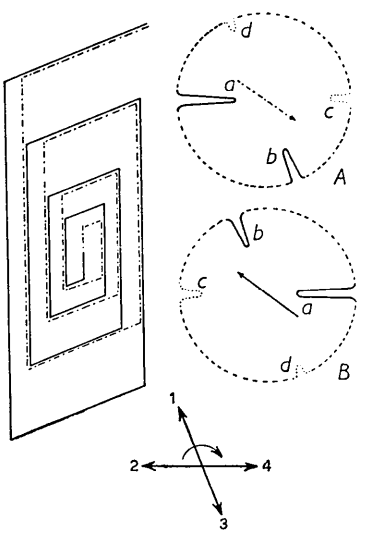

Fig. 7. Decomposition of the interlaced pattern of type 2 into single spirals.

In Fig. 1(*d*) the interlacing is somewhat different, but here, too, the polar diagrams for *A* and *B* are related by a rotation through 180°.

2·1·4. *Discussion and conclusions*

Without the knowledge of the structure, no detailed explanation can be given for the particular shape of the growth patterns. These observations suggest, however, that crystals of the orthorhombic form can be stacked in two ways. For one of them, the polar diagrams of successive monolayers are related by a mirror line, for the other by a rotation through 180°. These differences in stacking could, for example, be due to the two sets of hollows available on the limiting surfaces of a monolayer.

The whole of the growth pattern of type 1 has only

a line of symmetry; this is a very striking feature for the (001) face of an orthorhombic crystal. One would expect at least a twofold axis; this is in fact the case for the pattern of type 2.

2·2. *Growth promoted by imperfect dislocations in crystals of the n-alcohols (α- and β-form)*

2·2·1. *Introduction*

Growth originating at imperfect screw dislocations is accompanied by certain complications which we will now consider in some detail for the special case of polar long-chain molecules, which normally crystallize in double layers associated by means of their polar groups.

A dislocation whose Burgers vector is equal to an odd number of projected chain lengths is imperfect. The glide plane of such a dislocation is a misfit plane. When crossing this plane the stacking in any layer changes, as shown in Fig. 8, for the simple case where

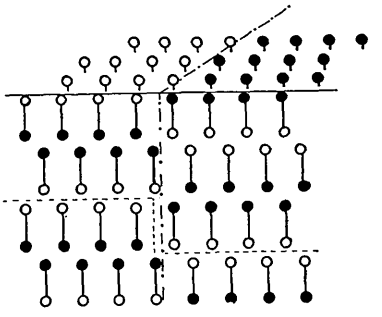

Fig. 8. Misfit surface associated with an imperfect dislocation in a polar long-chain crystal.

the chains are perpendicular to the basal plane.

In many cases the structure of the growth layer generated by the exposed edge of an imperfect dislocation is determined by the stacking present in this exposed edge; polytypes will then result and this is, for example, the case for SiC (Frank, 1951), mica (Amelinckx, 1952; Amelinckx & Dekeyser, 1952) and CdI_2 (Forty, 1952).

It is possible that this also applies to certain polar long-chain compounds, when the lateral bonding is strong. In such cases it is to be expected that the exposed edge of the imperfect dislocation will wind up into a simple spiral since the bottom monolayer is rate-determining, as it is highly hampered in its growth for two reasons:

(i) It has to grow by means of single molecules, whereas the bimolecular layers on it can grow by means of associated molecules as well.
(ii) There is misfit along the surface of the substrate layer.

This might explain the occurrence of non-integral steps on crystals of stearic acid, as observed by Verma & Reynolds (1953). These crystals would then be polytypic, with d_{001} equal to half-integral values of the normal repeat distance.

In other cases the substrate dictates the stacking, and the normal structure is continued but at the expense of some complications in the growth patterns. From our observations it will be clear that this is the case for the α-form of the *n*-alcohols, but we feel that this might be true for all long-chain compounds with strong polar end groups.

As shown by Anderson & Dawson (1953), polar long-chain crystals grow in certain circumstances (in polar solvents) by means of monomolecular layers or isolated molecules, and in other circumstances (in non-polar solvents) by means of bimolecular layers or associated molecules.

If a monomolecular step should be sufficient to promote the growth of a bimolecular layer, very typical growth patterns would result, which were, however, not observed. On the contrary, we observed patterns which are in agreement with the opposite assumption, i.e. that growth with bimolecular layers, starting at a monomolecular step, is not likely to occur.

From this it is clear that we will have to distinguish in our discussion between cases where growth proceeds with monolayers and cases where this is difficult or impossible.

2·2·2. *The imperfect dislocation is half the unit dislocation and growth with monolayers is possible*

Let us consider, for example, an orthorhombic crystal of the *n*-alcohols (α-form) containing a dislocation with a Burgers vector equal to one chain length. Suppose that the upper surface of the crystal consisted of CH_3 groups at the time when the dislocation was formed. Growth will start at the exposed edge AB of the dislocation and a monolayer front will be formed, the molecules having their OH groups upward. This is represented in Fig. 9 by the shaded

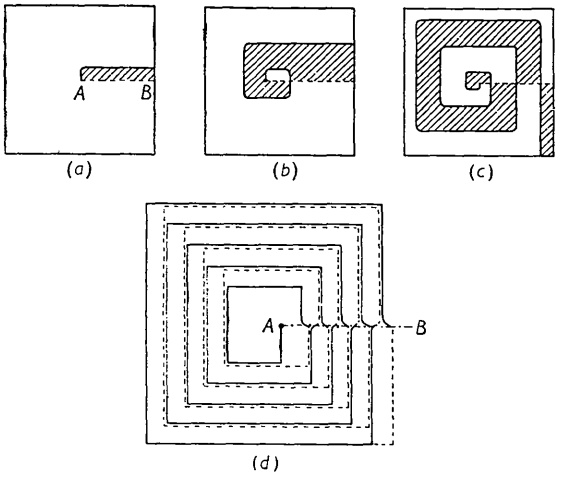

Fig. 9. Growth round a 'half' dislocation in a crystal of the orthorhombic form of *n*-alcohol.

area. In winding up, this front passes the trace of the misfit surface AB (i.e. the original position of the exposed edge). The growth layer now reaches a region where the upper surface is already formed by OH groups. In crossing the misfit line the stacking will have to change if the normal structure is to be continued; molecules will have again their CH_3 group upward (unshaded area of Fig. 9(*b*)). During continued winding up the stacking will have to change every time the line AB is crossed; the situation will thus be as shown in Fig. 9(*c*). Apparently nothing would reveal the change of stacking along the line AB. In reality, however, there may be differences in growth velocity for the different monolayers, as we have seen in § 2·1·2. The layer growing, for example, with the OH–OH binding will possibly be faster in one sector and slower in another; this will cause grouping into bimolecular fronts and interlacing, as shown in Fig. 9(*d*). As the stacking in the same layer changes along the line AB (i.e. the layer changes its name: — becomes ----), the rate-determining layer, which will become the lower one, will jump one chain length in level when crossing this line. This will lead to the formation of kinks, which, as a consequence, will mark the line AB. The pattern consists in fact of one single spiral, which nevertheless gives rise to an interlaced pattern.

Fig. 3 shows a growth pattern which has to be explained in the way described here.

2·2·3. *The imperfect dislocation is larger than the unit dislocation*

2·2·3·1. *Growth with monolayers thinner than the unit cell is difficult or impossible.*—This is the case for *n*-alcohols (β-form) in circumstances where growth proceeds mainly by means of bimolecular layers. Let us consider as an example a dislocation with a Burgers vector of 5 projected chain lengths. The exposed edge will give rise to two bimolecular spirals. The remaining monomolecular step will practically not be deformed by subsequent growth and will indicate the trace of the misfit surface. Every time the growing fronts cross this line there is a delay as the stacking in a given layer has to change; this causes a series of kinks. As in reality unassociated molecules will also be available in the solution, the monomolecular step will eventually advance also at a much smaller rate, but this changes nothing in what has been said above. Fig. 2(*b*) is an example, observed on the β-form of the *n*-alcohols. The fault line is partly monomolecular; the kinked parts, however, are three molecules high, whereas the growth fronts are bimolecular.

2·2·3·2. *Growth with monolayers.*—Let us consider as an example a dislocation with a Burgers vector of *five* chain lengths in a crystal of the α-form of the *n*-alcohols.

Five monomolecular spirals will now be developed. As a consequence of differences in growth velocity the fronts will be grouped, and interlacing will result. Along the misfit line the rate-determining layer will again jump one monolayer in level; this means that when crossing this line the slowest fronts become the fastest and vice versa. As a consequence a rearrangement of growth fronts of the type shown in Fig. 9 will take place along this line. This is quite clearly visible on Fig. 4(*a*) (α-form of alcohol), where five monomolecular spirals can be seen in the centre. The straight misfit line, which is parallel to the long diagonal, is clearly marked by the kinks.

2·2·4. *Growth originating at two imperfect dislocations of opposite sign*

Suppose for simplicity that both dislocations have a Burgers vector of one projected chain length. The misfit surface is now a portion of a plane limited by the two dislocation lines, and the misfit line connects their two emergence points.

When growth is possible the exposed edge now generates monolayer loops having their OH groups alternately upward and downward, the stacking changing every time the misfit line is crossed (Fig. 10).

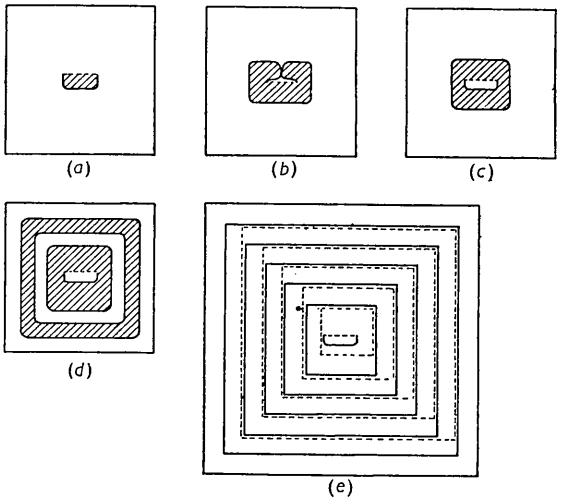

Fig. 10. Growth at two 'half' dislocations of opposite sign.

Again, interlacing will occur, but no kinks will be visible now, as generally no fronts cut the misfit line. An example (α-form of $C_{24}H_{49}OH$) is shown in Fig. 4(*b*). We do not consider the case when the two dislocations are larger than the unit dislocation. It is easy to derive the growth pattern in that case for growth with monolayers and with bimolecular layers.

2·2·5. *Imperfect dominated dislocations*

2·2·5·1. *Growth by means of bimolecular layers.*—The exposed edge associated with the dominated dislocation will remain unchanged. The advancing growth fronts will simply be split into two parts separated by the misfit line.

Along this line kinks will eventually be formed as a

consequence of the presence of the non-growing monomolecular step. This case has already been observed by Anderson & Dawson (1953) on crystals of stearic acid, and the correct interpretation was given. We mention it here only for completeness.

2·2·5·2. *Growth with monomolecular layers.*—The interaction of the growth fronts with the dominated half dislocation proceeds in approximately the same way as for perfect dislocations.

The original exposed edge AB is now the trace of a misfit plane, and the stacking in every lattice plane will be different on both sides of it. The interaction is schematized in Fig. 11, where in the shaded areas

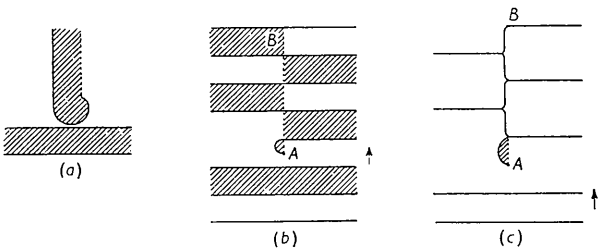

Fig. 11. Interaction of growth fronts with a dominated imperfect dislocation.

the OH groups are upward. After the passage of several fronts the situation is as shown in Fig. 11(*b*). Grouping of growth fronts will eventually take place as a consequence of differences in growth velocity. The final result will then be as shown in Fig. 10(*c*). Fig. 4(*c*) represents an example observed on a crystal of the α-form of the n-alcohol $C_{26}H_{53}OH$. The emergence point P of the dominated dislocation is marked by an arrow; the zigzag line starting in P is clearly visible.

2·2·5·3. *Other growth patterns due to imperfect dislocations.*—We will now analyse a somewhat more complicated pattern necessitating the presence of imperfect dislocations.

In Fig. 2(*a*) ($C_{24}H_{49}OH$, β-form) a straight line cutting growth fronts is visible.

Starting with a dislocation having an exposed edge partly three and partly four chain lengths high, as shown in Fig. 12, and taking into account that growth proceeds with bimolecular layers, this pattern can be explained in a logical way.

The dislocation in A is imperfect (as the exposed edge is $1\frac{1}{2}$ unit cells high). From B on the exposed edge is 2 unit cells high. A bimolecular spiral will thus be centred on A and another one on B (Fig. 12(*b*)); moreover, a non-growing monomolecular step will connect A and B.

After one complete turn, part of the front of spiral A coincides again with the original line AB. This small part of the spiral step is three molecules high, and after a small delay caused by the change in stacking it can grow further. The spiral A develops normally except for the small discontinuity which occurs on every crossing of the line AB.

This, however, is not so for B. When half a turn is developed, part of the bimolecular front meets the non-growing monomolecular step, leaving only a monomolecular step in the reversed sense. This step is incapable of promoting growth; consequently the spiral step emerging in B can only move along the line AB

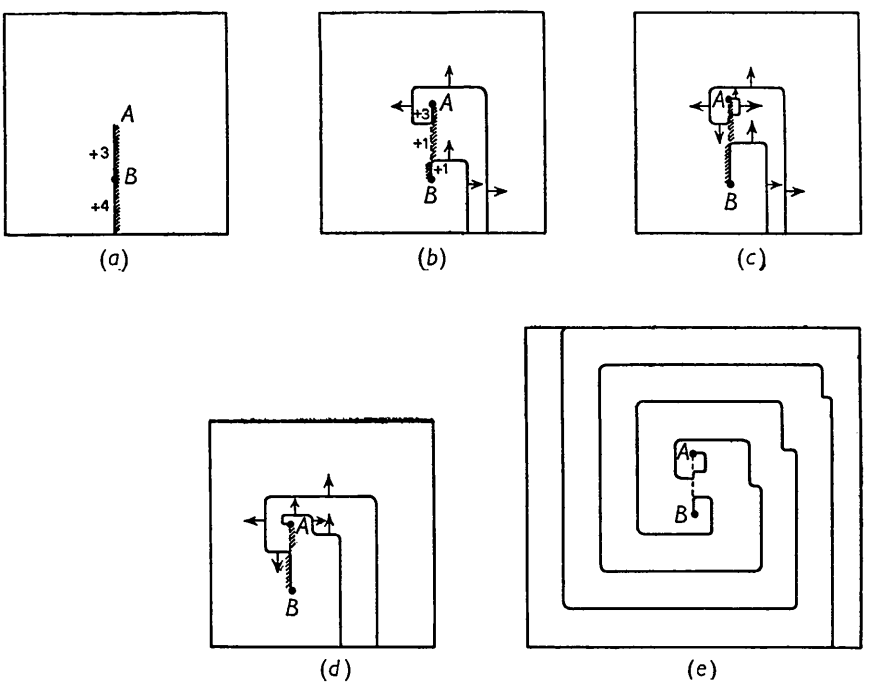

Fig. 12. Growth round an imperfect dislocation in crystal of the β-form of n-alcohols.

until it meets the right part of the front of spiral A. At that moment they exchange centres, and, after some further growth, the left part of spiral A will be attached to the centre B and the cycle starts again (Fig. 12(d)). The final result will be Fig. 12(e), which can be compared directly with Fig. 2(a).

More growth patterns involving the presence of imperfect dislocations, which occur relatively frequently in long-chain crystals, were observed, but this single example will be sufficient to illustrate the way in which they can complicate growth patterns.

3. Twins in n-alcohols and n-carboxylic acids

3·1. *Introduction*

Although growth features on crystals of monocarboxylic acids will be treated in Part III, we describe here the twinning of these crystals, as there is a close relation with the twinning of n-alcohols.

3·2. *Monoclinic (β) form of n-alcohols*

A crystallographic description of the single crystals of n-alcohols is given in Part I.

3·2·1. *Crystallography of twins*

Crystals of this modification often grow as contact twins along their c(001) face (Figs. 5(b) and 13(a)).

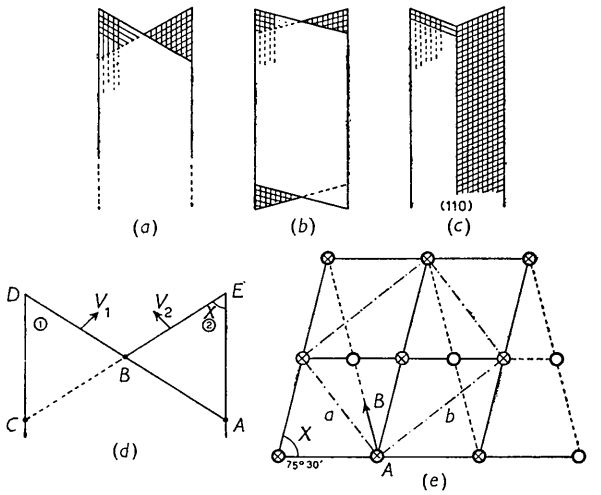

Fig. 13. (a) Contact twin of the β-form of n-alcohols.
(b) Contact twin of the B-form of monocarboxylic acids.
(c) Contact twin of the α-form of n-alcohols.
(d) Illustrating the growth mechanism of twins of type (a).
(e) Lattice points on both sides of the contact plane of the twin of type (b).

The individual crystals are very frequently only a few bimolecular layers thick, and in most cases they do not exhibit growth steps, proving their growth to be by means of two dimensional nucleation.

The absence of growth fronts makes it impossible to compare the tilt directions of the chains on both individuals. It is thus not possible to deduce unambiguously the symmetry relation between the two crystals. The first possibility would be that individual crystals are turned one with respect to the other through 120° round an axis normal to c(001). In that case the twin elements would be: contact plane: (001); twin axis: [110].

The second possibility is a relative rotation of 60° about the normal to (001). The twin elements would then be: contact plane: (001); twin axis: normal to [110] and situated in (001) (when, assuming $\chi = 60°$, this is $[1\bar{3}0]$).

Taking into account the considerations of § 2·2 of Part I concerning the structure of the limiting surfaces of a bimolecular layer, the occurrence of this kind of crystal assembly is quite natural, and both possibilities are likely to occur. It is further to be expected that crystal assemblies where the individuals are turned relatively through an angle $\varphi = 180°$ will also occur. These, however, cannot be distinguished from simple crystals by means of the microscope. Their twin elements would be: contact plane: (001); twin axis: normal to (001).

3·2·2. *Mechanism for lateral growth of twins*

A remarkable and constant feature of the twins described in § 3·2·1 is the elongation in the direction of the concave angle and the approximately equal development of the two tips D and E (Fig. 13(d)). A simple growth mechanism accounts for these particularities.

Crystal (1) will grow in the direction normal to AD by means of layers nucleated at the step AB, whilst crystal (2) will grow in the direction normal to EC by nucleation along the step BC. The probability of forming a new row (or layer) of molecules will evidently be larger, the greater the length of these steps. The simplest assumption is to put

$$v_1 = ax; \quad v_2 = ay\,, \tag{1}$$

where a is an arbitrary proportionality factor, $x = AB$ and $y = BC$, and v_1 and v_2 are the normal growth rates of AB and BC respectively. This assumption will only be justified if the inclination of the chains has the same sense along AD and CE.

From Fig. 13(d) it is immediately evident that the increase in x as a consequence of the displacement of BC is

$$v_2 \Delta t \operatorname{cosec} 2\alpha = m v_2 \Delta t\,,$$

whilst the decrease of x as a consequence of the movement of AB is

$$v_1 \Delta t\,(\cot 2\alpha - \cot \alpha) = n v_1 \Delta t\,.$$

We thus have

$$dx/dt = m v_2 + n v_1$$

and similarly

$$dy/dt = m v_1 + n v_2\,.$$

From (1) the following set of differential equations results:

$$dx/dt = may+nax,\ dy/dt = max+nay\ . \qquad (2)$$

The ratio x/y can be calculated from (2); one has

$$du/dt = ma(1-u^2);\ \ u = x/y\ ,$$

and consequently

$$u = [1+u_0 \exp(-2amt)]/[1-u_0 \exp(-2amt)]\ , \qquad (3)$$

u_0 being an integration constant. For $\chi = 59°$, m is positive. Formula (3) proves then that the final equilibrium development will be such that $u = 1$; i.e. $x = y$ even when starting with $u_0 \neq 0$.

If the inclination of the chains is different along AD and CE, (1) becomes

$$v_1 = ax,\ \ v_2 = by\ .$$

The equilibrium development will now be given by

$$x/y = b/a\ . \qquad (4)$$

We have here a good example of an instance where growth is facilitated during an *unlimited* period, *without* the aid of dislocations.

3·3. *Orthorhombic form of n-alcohols*

Contact twins of the shape represented by Fig. 13(*c*) are frequent. Twin elements are: contact plane: (110); symmetry plane: (110). These twins are due to a stacking fault in the lateral growth of a layer. They are also elongated in the direction of the concave angle. Dawson (1952) observed similar twins in *n*-hectane. He explained their particular shape as a result of preferential nucleation in the concave angle.

3·4. *Carboxylic acids: B-form*

On crystals of the *B*-form contact twins of the type represented in Fig. 13(*b*) are observed. As a consequence of the inclination of the chains two different twin laws (as in the case of the *n*-alcohols) are to be considered: contact plane: *c*(001); twin axis: either [110] or the direction perpendicular to it.

The considerations of § 3·1·2 concerning the growth mechanism can, of course, also be applied here.

In the case of the *n*-alcohols the 'twin' positions were in a clear relation to the structure of the limiting surface of a bimolecular layer. In the present case this relation is less evident. Fig. 13(*e*) represents the lattice points in the planes on both sides of the contact plane. It is shown that for an angle of $\chi = \text{arc cos}\frac{1}{4} = 75°\ 30'$ there would be coincidence over half the number of lattice points. A translation of the lattice of the small circles over the vector AB, with respect to the lattice of the 'crossed' circles, would bring the circles into the 'hollows' of the crosses. Whereas in the normal stacking all the 'hollows' of one kind would be occupied, half of the hollows of every kind will be filled now.

The real value of χ is 74°, but this angle varies somewhat from crystal to crystal, and in the case of twin crystals it is in fact often somewhat larger. The relatively good fit for the two planes is the reason why stacking faults, and consequently twins, are so easily formed.

3·5. *The growth of macroscopic twins*

In the preceding paragraphs we have considered twin crystals only a small number of molecular layers thick, and showing no growth steps. We will now consider what would happen to such a crystal assembly presenting a screw dislocation after further growth. Two different possibilities arise: either an ordinary macroscopic twin or a polysynthetic twin can result.

3·5·1. *Ordinary twins*

When the Burgers vector of the screw dislocation has a component perpendicular to *c*(001) smaller than the thinnest crystal of the assembly, each individual will grow following its own orientation. On the upper and lower face of the crystal growth spirals will be developed; they will be in twin orientation as well as the crystals themselves. An example, observed on a crystal of the *B*-form of lignoceric acid, is visible in Fig. 5(*c*).

3·5·2. *Polysynthetic twins*

When, on the contrary, the Burgers vector has a component perpendicular to (001) exceeding in length the thickness of the thinnest of the individual crystals, layers in both orientations will be exposed on the thinnest crystal.

Further growth on this crystal will generate an assembly consisting of a regular alternation of lamellae in twin position; this is commonly called a *polysynthetic twin.*

If the screw dislocation is so large as to expose layers in both orientations also on the thickest crystal, polysynthetic twins will result on both sides of the original contact plane. Implications of this mechanism are of course that successive lamellae of the same orientation should have constant thickness, and further that the contact plane should be a habit face. These conditions are *not* fulfilled for many polysynthetic twins. It is therefore *not* claimed that this mechanism applies to all polysynthetic twins.

The present mechanism for the growth of polysynthetic twins was already suggested earlier (Amelinckx, 1952) but no example could be offered at that time. An example observed on the *B*-form of behenic acid is shown in Fig. 5(*a*). The individuality of both helicoidally wound crystals is accentuated by the fact that one lamella grows over the edge of the underlying one. The two tips (*D* and *E* of Fig. 13(*d*)) are not equally developed, but the lengths of BE and DB are approx-

imately in a constant ratio. This can most simply be explained by the assumption of a difference in inclination of the chains along the edges of the concave angle; in this case formula 3·2·2·(4) applies.

3·6. *Discussion*

It is evident that the mechanism here proposed for *polysynthetic twinning* is in fact equivalent to the one for *polytypism*. It would as a consequence be justified, in a certain sense, to call the crystal of Fig. 5(*a*) a polytype. For the β-form of the n-alcohols the relation between twinning and polytypism (Part I) is even more striking: twin formation as well as polytypism are both direct consequences of the different stacking possibilities of successive bimolecular layers.

The author is grateful to Prof. W. Dekeyser for the stimulating interest taken in this work, which is part of a research programme (Centre pour l'étude de l'État Solide) supported by I. R. S. I. A. (Institut pour l'encouragement de la Recherche Scientifique dans l'Industrie et l'Agriculture).

References

AMELINCKX, S. (1951). *J. Chim. Phys.* **48**, 1.
AMELINCKX, S. (1952). *C. R. Acad. Sci., Paris*, **234**, 971.
AMELINCKX, S. (1955). *Acta Cryst.* **8**, 530.
AMELINCKX, S. & DEKEYSER, W. (1952). *Comptes Rendus de la 19e Session du Congrès Géologique international*, **18**, 9.
ANDERSON, N. G. & DAWSON, I. M. (1953). *Proc. Roy. Soc.* A, **218**, 255.
DAWSON, I. M. (1952). *Proc. Roy. Soc.* A, **214**, 72.
FORTY, A. J. (1952). *Phil. Mag.* (7), **43**, 72.
FRANK, F. C. (1951). *Phil. Mag.* (7), **42**, 1014.
TOLANSKY, S. (1948). *Multiple-Beam Interferometry of Surfaces and Thin Films*. Oxford: Clarendon Press.
VERMA, A. R. & REYNOLDS, P. M. (1953). *Proc. Phys. Soc.* B, **66**, 414.

Acta Cryst. (1956). **9**, 23

The Geometrical Basis of Crystal Chemistry. Part 6

BY A. F. WELLS

Imperial Chemical Industries Limited (Dyestuffs Division), Hexagon House, Manchester 9, *England*

(*Received* 4 *July* 1955)

In Part 1 it was stated that the only three-dimensional 3-connected nets of the n^3 type are 8^3, 9^3 and 10^3, and that there are two different nets corresponding to the symbol 8^3 and similarly for 10^3. It is now shown that there are also nets 7^3, as well as further nets 8^3, 9^3 and 10^3. These new nets are derived in a systematic way and illustrated.

Three-dimensional 3-connected nets related to the regular solids

Part 1 (Wells, 1954*a*) dealt with the systematic derivation of periodic three-dimensional 3-connected nets containing 4 or 6 points in the repeat unit. It was noted that certain of these nets are related to the three regular solids which have three edges (faces) meeting at each vertex. The symbols 3^3 (tetrahedron), 4^3 (cube), and 5^3 (pentagonal dodecahedron) indicate that three 3-gons, 4-gons, or 5-gons respectively meet at each vertex. The next number of this n^3 series is the plane hexagonal net (6^3), and it was remarked that the series is continued by the three-dimensional nets 8^3, 9^3 and 10^3. Some of these were described and illustrated in Part 1, where it was stated: 'It would seem, though this point has not been proved, that the only nets of the n^3 type are 8^3, 9^3 and 10^3, and that there are two different nets corresponding to the symbol 8^3, and similarly for 10^3'. The purpose of the present paper is to show that, in fact, there are also nets 7^3, as well as further nets 8^3, 9^3 and 10^3, so that the series is complete from 3^3 to 10^3.

We shall require (1) that each point is connected to three others, and (2) that there must be a configuration of each net in which the distance between any pair of unconnected points is greater than the distance between any pair of connected points. Since we are interested in the three-dimensional 'homologues' of the 3-connected regular solids we shall also insist (3) that there must be a possible configuration of a net having all links equal in length. (This condition was not explicitly laid down in Part 1; it is related to (2) above, and it is possible that it has been implicitly assumed in Parts 1 and 2.)

In the systems 3^3, 4^3 and 5^3, and the strictly planar regular form of 6^3, it is sufficient to describe the polygons as equilateral *or* equiangular, since a regular plane polygon has both these properties, and all the polygons in a given system are congruent. In the three-dimensional nets we shall consider here the polygons are not plane, and it is possible to have configurations